# Diatom $\delta^{18}O$ evidence for the development of the modern halocline system in the subarctic northwest Pacific at the onset of major Northern Hemisphere glaciation

George E. A. Swann,[1] Mark A. Maslin,[1] Melanie J. Leng,[2,3] Hilary J. Sloane,[2] and Gerald H. Haug[4]

Received 17 February 2005; revised 22 July 2005; accepted 18 November 2005; published 24 February 2006.

[1] Establishing a time frame for the development of the modern halocline and stratified water column in the subarctic North Pacific has significant paleoclimatic implications. Here we present a $\delta^{18}O_{(diatom)}$ record consisting of only two species that represents autumn/winter conditions in the region across the onset of major Northern Hemisphere glaciation boundary. At circa 2.73 Ma a decrease in $\delta^{18}O_{(diatom)}$ of 4.6‰ occurs, whereas previously published $\delta^{18}O_{(foram)}$ results show a 2.6‰ increase. The $\delta^{18}O_{(diatom)}$ and $U^{k}_{37}$ sea surface reconstructions indicate both a significant freshening of 2–4 practical salinity units and an increase in surface temperatures in the summer to early winter period from circa 2.73 Ma onward. In contrast, the concomitant increase in $\delta^{18}O_{(foram)}$ is likely to be reflective of conditions beneath the mesothermal structure and/or spring conditions when warmer sea surface temperatures are not present in the region. These results are consistent with the development of the modern halocline system at 2.73 Ma with year-round stratification of the water column and a strengthened seasonal thermocline during the summer to early winter period, resulting in one of the largest summer to winter temperature gradients in the open ocean. The onset of stratification would also have led to a warm pool of surface water from circa 2.73 Ma, which may have provided a potential source of extra moisture needed to supply the growing North American ice sheets at this time.

**Citation:** Swann, G. E. A., M. A. Maslin, M. J. Leng, H. J. Sloane, and G. H. Haug (2006), Diatom $\delta^{18}O$ evidence for the development of the modern halocline system in the subarctic northwest Pacific at the onset of major Northern Hemisphere glaciation, *Paleoceanography*, *21*, PA1009, doi:10.1029/2005PA001147.

## 1. Introduction

[2] The onset of major Northern Hemisphere glaciation (NHG), marking the large-scale expansion of ice sheets from circa 2.75 Ma, represents a significant climatic transition during the prolonged period of global climatic cooling initiated with the late Miocene glaciations of the Northern Hemisphere [*Zachos et al.*, 2001; *Kleiven et al.*, 2002]. *Ravelo et al.* [2004] suggests that the onset of major NHG was part of a series of climatic changes which started with gradual cooling at circa 4 Ma and included the intensification of the Walker circulation at circa 2 Ma and the mid-Pleistocene revolution at circa 0.9 Ma. The precise mechanisms behind the initiation of NHG remain uncertain with lower summer isolation at 65°N, related to changes in obliquity from circa 3.2 Ma and precession from circa 2.8 Ma [*Haug and Tiedemann*, 1998; *Li et al.*, 1998; *Maslin et al.*, 1998], unable alone to force the growth and maintenance of glaciers across the Northern Hemisphere. Uplift and subsequent tectonic induced chemical weathering of the Tibetan/Himalayan plateau [*Ruddiman and Raymo*, 1988; *Raymo*, 1994] and increased volcanic activity in the Kamchatka-Kurile and Aleutian arcs [*Prueher and Rea*, 2001] have all been proposed, in conjunction with variations in summer isolation, to explain the establishment of cooler conditions. In addition to climatic cooling though, an essential prerequisite for the development of glaciers across the Northern Hemisphere is a significant increase in the supply of moisture to the growing ice sheets. The most viable mechanism to provide this to Eurasia/Arctic is through the closure of the Panama gateway between 4.6 Ma and 1.8 Ma and consequential oceanic/atmospheric changes associated with alterations in the strength of the Gulf Stream [*Haug and Tiedemann*, 1998; *Haug et al.*, 2001; *Lear et al.*, 2003]. This though does not resolve the unexplained problem of how increased moisture was delivered to the Alaskan and North American ice sheets over the same interval.

[3] To date, the role of the subarctic Pacific Ocean across the onset of major NHG has been largely ignored despite the role of the modern day region in providing moisture to Northern America [e.g., *Koster et al.*, 1986; *Bosilovich*, 2002]. The region is dominated by the cyclonic Alaskan subpolar gyre bordered to the south by the North Pacific Current (also called the Subarctic Current and West Wind Drift) and to the North by the Alaska Stream (Figure 1). The

[1] Environmental Change Research Centre, Department of Geography, University College London, London, UK.
[2] NERC Isotope Geosciences Laboratory, British Geological Survey, Nottingham, UK.
[3] School of Geography, University of Nottingham, Nottingham, UK.
[4] Geoforschungszentrum Potsdam, Potsdam, Germany.


0883-8305/06/2005PA001147$12.00

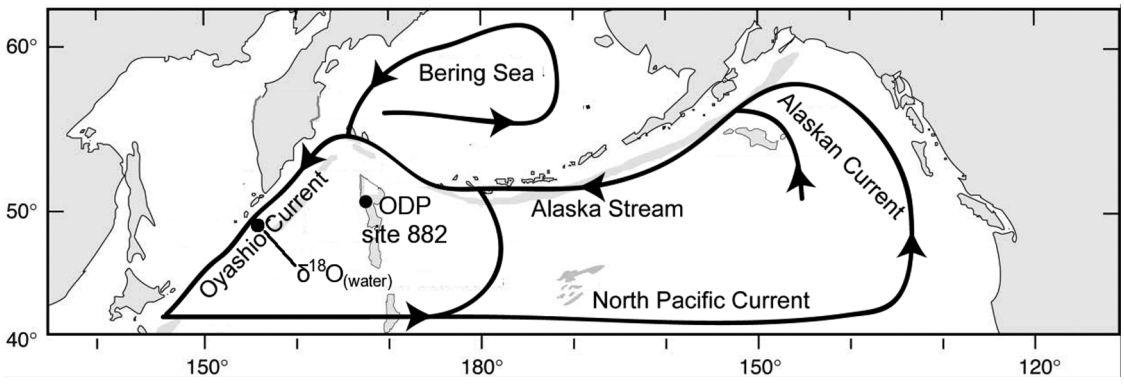


**Figure 1.** Location of Ocean Drilling Program (ODP) site 882 (50°22'N, 167°36'E) northwest subarctic Pacific together with major ocean surface currents in the North Pacific and the location of $\delta^{18}O_{(water)}$ values displayed in Figure 2 (49.12°N, 156.25°E).

northwest subarctic Pacific also marks the terminus of the North Pacific Deep Water (NPDW), the final sector of the deep ocean section of the global thermohaline circulation, with the upwelling of nutrient rich NPDW to the subsurface forming North Pacific Intermediate Water (NPIW). Today, the water column in the northwest subarctic Pacific is marked by a highly stable surface ocean stratification driven by a deep, 150–200 m, year-round halocline marked by surface waters of approximately 32.8 practical salinity units (psu) (Figure 2). From June to December, the stratification is further enhanced by the presence of a shallower, approximately 50 m, thermocline in which sea surface temperatures (SST) of approximately 9°–10°C (Figure 2) can exist until December. In contrast, waters below the thermocline are closer to 2°C. The oceanographic mechanisms which create and maintain this mesothermal structure have been an area of intensive research leading to the suggestion of several different processes that focus on the role of particularly high precipitation in the region and differential horizontal advection within the water column [see *Gargett*, 1991; *Ueno and Yasuda*, 2000]. A detailed review of these mechanisms is discussed by *Ueno and Yasuda* [2000].

[4] ODP site 882 (Figure 1) in the northwest Pacific provides the first detailed paleoclimatic record in the region from the late Miocene onward enabling key insights into the system both before, during and after beginning of NHG [*Rea et al.*, 1995]. Today, the biological community in the northwest Pacific is marked by the year-round presence of foraminifera in the water column, particularly during spring and to a smaller extent during the autumn/early winter months [*Kuroyanagi et al.*, 2002; *Mohiuddin et al.*, 2005].

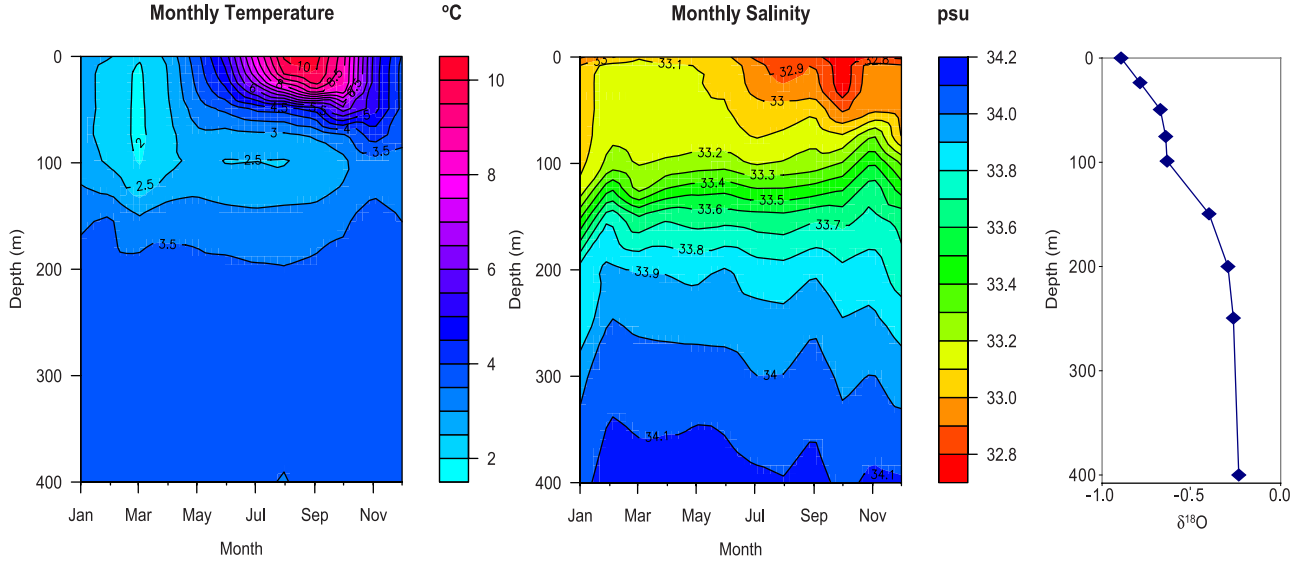


**Figure 2.** Modern salinity and temperature depth profiles in the upper 400 m of the subarctic northwest Pacific (50.5°N, 167.5°E) [*Boyer et al.*, 2002; *Stephens et al.*, 2002] with $\delta^{18}O_{(water)}$ values from 49.12°N, 156.25°E (G. A. Schmidt et al., Global seawater oxygen-18 database, 1999, available at http://data.giss.nasa.gov/o18data/).

During the spring months, however, the photic zone is primarily dominated by a large siliceous bloom containing a number of diatoms species and additional smaller contributions from silicoflagellates [*Onodera and Takahashi*, 2005]. In the summer months, when concentrations of phytoplankton in the surface mixed layer are reduced, dinoflagellates increase in abundance in the water column [*Mochizuki et al.*, 2002]. At no point though does nutrient limitation prevent phytoplankton growth [*Mochizuki et al.*, 2002]. From the late summer to early winter period, a second diatom bloom occurs but at concentrations below that experienced during the spring bloom [*Takahashi*, 1986; *Takahashi et al.*, 1996; *Onodera and Takahashi*, 2005]. In some years, however, conditions exist to cause the autumnal diatom bloom to be of an equal magnitude to that experienced during the spring bloom [*Onodera and Takahashi*, 2005]. During this second bloom, high levels of coccolithophores also develop within the photic zone which results in the accumulation of alkenones within the sedimentary record [*Ohkouchi et al.*, 1999; *Pagani et al.*, 2002].

[5] Prior to NHG, circa 2.73 Ma, high, approximately 70 g $cm^{-2}$ $kyr^{-1}$, opal concentrations are recorded in the sediment at ODP site 882 [*Haug et al.*, 1999]. The supply of high nutrient concentration necessitated for this can only be obtained by significant upwelling of nutrient rich NPDW to the photic zone, suggesting the lack of a stratified system prior to this period [*Haug et al.*, 1999]. Such a scenario is not feasible in the modern ocean with the halocline restricting the supply of NPDW to the mixed layer, which rarely extends beyond 150 m (Figure 2). Instead today, nutrient supply to the photic zone is predominantly restricted to limited diffusion through the stratified water column [*Tabata*, 1975; *Gargett*, 1991]. The development of the modern halocline at ODP site 882 has therefore previously been related to the development of the NHG at circa 2.73 Ma, when opal mass accumulation rates (MAR) decrease threefold and $\delta^{15}N_{(bulk\ sediment)}$ increases by approximately 2‰ [*Haug et al.*, 1999; *Sigman et al.*, 2004]. Accordingly, at the onset of NHG, autumn/early winter SST would be expected to increase following the development of a stratified water column, despite the presence of globally cooler conditions, because of the halocline and thermocline temperature inversion. In the modern ocean these factors results in unusually warm SST between June/July and December (Figure 2).

[6] Without the presence of a stratified water column, the build up and maintenance of a warm pool of water would be untenable because of the strong vertical mixing between the surface and subsurface layers with the upwelling of the cold NPDW. At the onset of major NHG, SST in the region would therefore be expected to decrease in an open, unstratified, system. Suggestions that the modern halocline system in the region developed at circa 2.73 Ma [*Haug et al.*, 1999; *Sigman et al.*, 2004] are therefore disputed by the presence of a 7.5°C cooling signal in $\delta^{18}O_{(foram)}$ between 2.75 Ma and 2.73 Ma [*Maslin et al.*, 1995, 1996]. To resolve the existing conflicting records over this period and to fully attain whether the modern day halocline system developed in the region at the onset of major NHG, circa 2.73 Ma, a conclusive record is required of autumnal changes in sea surface salinity (SSS) and SST.

[7] Analysis of $\delta^{18}O_{(diatom)}$ represents a technique holding significant potential for reconstructing past environmental change in regions depleted in $CaCO_3$ fossils. So far, studies have only taken full advantage of $\delta^{18}O_{(diatom)}$ between the Holocene and MIS 5e [e.g., *Mikkelsen et al.*, 1978; *Shemesh et al.*, 1992; *Morley et al.*, 2005; *Leng and Barker*, 2006]. Here we have analyzed $\delta^{18}O_{(diatom)}$ in pure diatom samples from ODP site 882 which are dominated by only two species, both of which bloom in autumn/early winter. In conjunction with newly published $U^{k}_{37}$ data [*Haug et al.*, 2005], this record provides clear and reliable evidence of autumn to early winter condition in the northwest subarctic Pacific between circa 2.8 Ma and circa 2.4 Ma. By combining the two records together to calculate changes in SSS, we obtain definitive evidence of a significant decrease in SSS in the region at the onset of major NHG which is consistent with the development of a halocline system in the region.

## 2. Methodology

[8] Sediment samples were collected from the northwest Pacific, Ocean Drilling Project (ODP) site 882, situated on the western section of the Detroit Seamounts (50°22′N, 167°36′E) at a water depth of 3,244 m (Figure 2) [*Rea et al.*, 1995]. High-resolution GRAPE density and magnetic susceptibility measurements were astronomically calibrated to provide an age model for the last 4 Ma [*Tiedemann and Haug*, 1995] with linear interpolation of sedimentation rates between the astronomical tie points used to calculated sample ages in this study.

[9] Samples for $\delta^{18}O_{(diatom)}$ were prepared using a three-stage methodology based on the techniques of *Juillet-Leclerc* [1986], *Shemesh et al.* [1995], and *Morley et al.* [2004] (Figure 3). Material was sieved at 75 μm and 150 μm with both size fraction (75–150 μm and >150 μm) retained for isotope analysis. Visual inspection of the diatom flora prior to this stage showed the 75–150 μm and >150 μm fraction sizes as being optimal to minimize diatom species diversity while also ensuring removal of clay and other nondiatom material. Both size fractions were subsequently immersed in 30% $H_2O_2$ at 80°C for several hours to remove organic matter attached to the diatom frustule. Samples were subsequently centrifuge washed and placed overnight in 5% HCl to remove carbonate material. Following further centrifuge washing, samples were resieved at their respective size fractions to remove any remaining contamination and smaller diatoms before being placed in a drying cabinet. Samples younger than circa 2.7 Ma required the use of a vortex mixer to separate diatoms from the heavier ice-rafted debris (IRD) prior to the final sieving stage. Subsamples of the final purified material were mounted on a coverslip using a Naphrax® mounting media and visually checked for contamination under a light microscope at 1000 times magnification following the semi-quantitative approach of *Morley et al.* [2004] but using

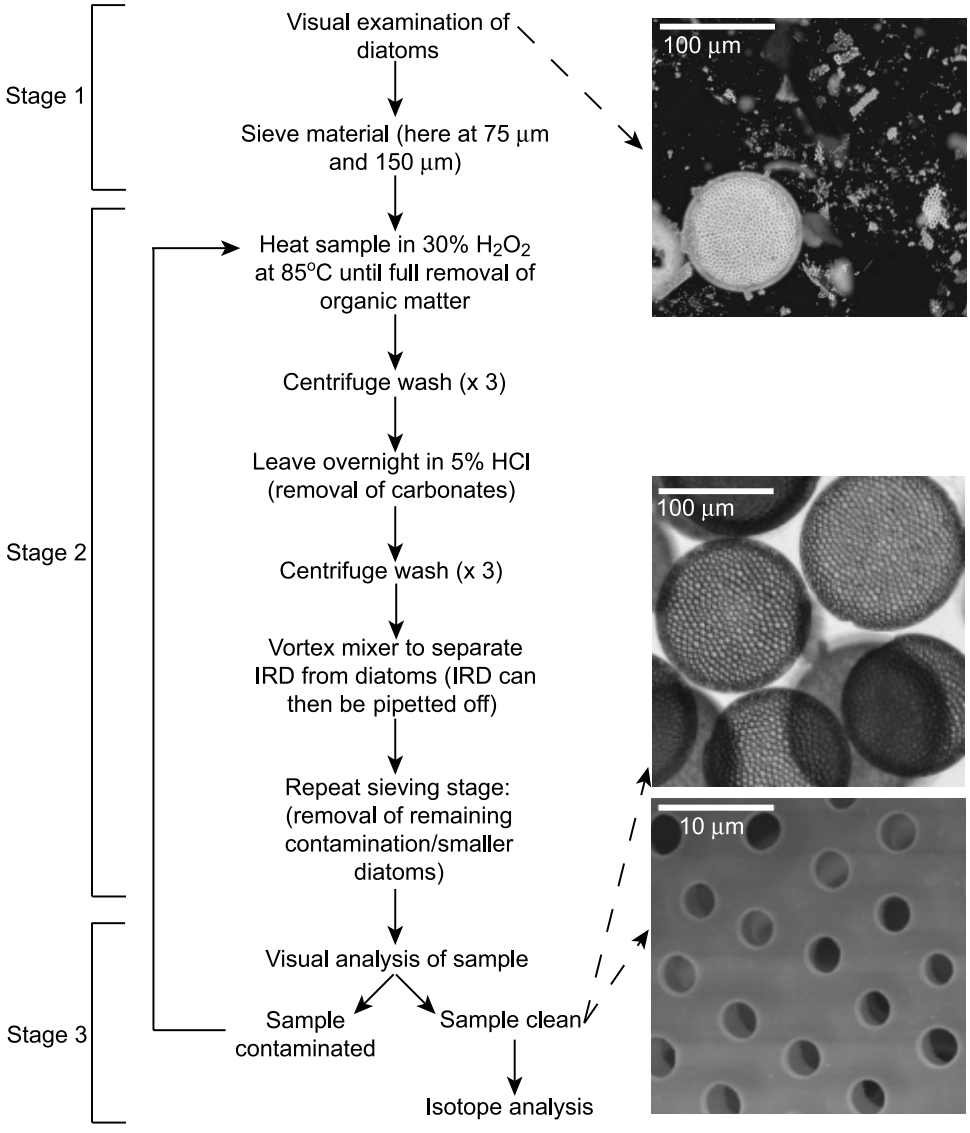


**Figure 3.** Three-stage methodology used to extract pure diatom material for oxygen isotope analysis based upon the methodologies described by *Juillet-Leclerc* [1986], *Shemesh et al.* [1995], and *Morley et al.* [2004]. Stage one utilizes the physical properties of different species to extract a small range of diatom species that all bloom in a single season, minimizing any potential interspecies fractionation and/or seasonal effects. Stage two chemically removes organic matter attached to the diatom frustule and any carbonates in the sample. Stage three verifies the purity of the diatom sample prior to isotope analysis.

30 rather than 10 randomly selected quadrants on a 100 μm × 100 μm grid graticule. Further SEM analysis was undertaken to ensure sample purity. Samples containing more than a few percent of nondiatom material were disregarded for isotope analysis. Diatom species biovolumes were calculated using the recommendations of *Hillebrand et al.* [1999].

[10] Diatom hydrous layers were stripped during a prefluorination outgassing stage in nickel reaction tubes using a stoichiometric deficiency of $BrF_5$ reagent at low temperature before full reaction with an excess of reagent at high temperature. Oxygen was converted to $CO_2$ following the methodology of *Clayton and Mayeda* [1963] with $\delta^{18}O_{(diatom)}$ measured on an Optima dual inlet mass spectrometer. The $\delta^{18}O_{(diatom)}$ values were converted to the SMOW scale using a within-run laboratory standard ($BFC_{mod}$) calibrated against NBS28. Replicate analysis of sample material indicated a $\delta^{18}O_{(diatom)}$ reproducibility of between 0.1‰ and 0.4‰, mean = 0.3‰.

## 3. Results

[11] All samples analyzed for $\delta^{18}O_{(diatom)}$, with the exception of one sample at 2.42 Ma, were over 96% free of nondiatom material with over half of all samples at least 99% pure (Figures 4 and 5). We calculated that a 4% contamination level will only alter the $\delta^{18}O_{(diatom)}$ signal

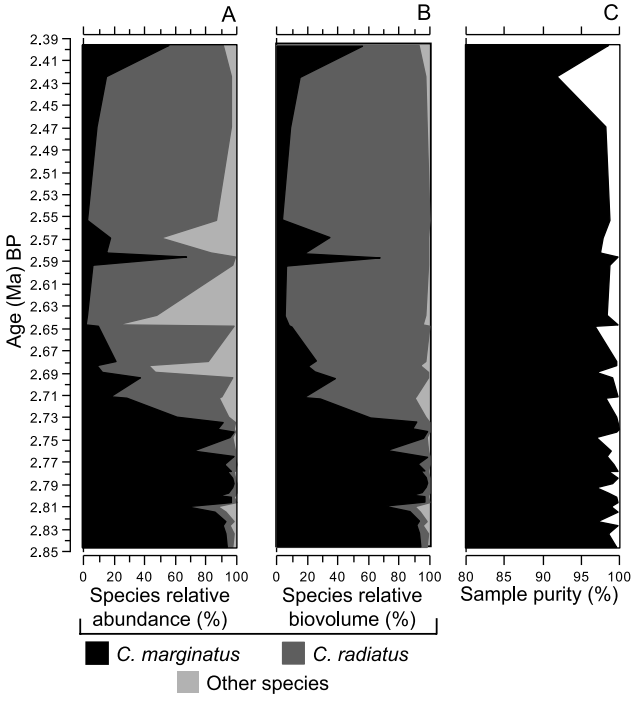


**Figure 4.** (a) Diatom species relative abundance in samples analyzed for $\delta^{18}O_{(diatom)}$ at ODP site 882 between 2.85 Ma and 2.35 Ma following sample preparation. (b) Diatom species percentage biogenic silica biovolume, relative to total biogenic silica biovolume, in samples analyzed for $\delta^{18}O_{(diatom)}$. (c) Sample purity, percentage of diatom material relative to all other material, in samples analyzed for $\delta^{18}O_{(diatom)}$.

within error of the analysis. Between 2.85 Ma and 2.73 Ma diatom assemblages were dominated by 60–99% abundance of *Coscinodiscus marginatus* (Ehrenb.) with the remainder principally made up of *Coscinodiscus radiatus* (Ehrenb.) (Figure 4). After circa 2.73 Ma the relative abundances of *C. radiatus* and *C. marginatus* are reversed except for five samples between circa 2.69 Ma and 2.57 Ma where the proportion of other species increases to over 40% abundance. Calculation of diatom species biogenic silica biovolume however shows the influence of these other species to be minimal, constituting on average less than 2.2% of the total volume of biogenic silica analyzed for $\delta^{18}O_{(diatom)}$ (Figure 4). Consequently, $\delta^{18}O_{(diatom)}$ can be regarded in this study as being representative of oxygen isotopes in only two diatom species, *C. radiatus* and *C. marginatus*, with minimal influence imparted by other species. Annual maximum fluxes of both *C. marginatus* and *C. radiatus* occur in the autumn/winter period [*Takahashi*, 1986; *Takahashi et al.*, 1996; *Onodera et al.*, 2005; K. Takahashi and J. Onodera, personal communication, 2005) (Figure 6) indicating the $\delta^{18}O_{(diatom)}$ signal obtained throughout this study to be representative of these conditions. Analysis of the $\delta^{18}O_{(diatom)}$ signal in both the 75–150 μm and >150 μm size fraction at three different levels between 2.83 and 2.73 Ma reveal similar results (Figure 7). At these levels, the 75–150 μm fractions are dominated by *C. marginatus* with minimal numbers of *C. radiatus*. Opposite relative abundances exist in the >150 μm fraction indicating the lack of interspecies vital effects between these two taxa (Figure 7).

[12] Analysis of $\delta^{18}O_{(diatom)}$ from the 75–150 μm size fraction reveals minor fluctuations between 43.4‰ and 44.8‰ from 2.83 Ma to 2.74 Ma following an initial increase of 1.5‰ between 2.85 Ma and 2.83 Ma (Figure 8). At 2.73 Ma, $\delta^{18}O_{(diatom)}$ decreases by 4.6‰ before 2.71 Ma. A rapid 1.7‰ increase in $\delta^{18}O_{(diatom)}$ is observed over the next approximately 2000 years before values decrease to 38‰ at 2.70 Ma. Sharp oscillations of approximately 8‰ characterize the $\delta^{18}O_{(diatom)}$ record between 2.70 Ma and 2.64 Ma before $\delta^{18}O_{(diatom)}$ becomes more positive from 37.1‰ to 42.6‰ over the subsequent 86,000 years with a short-lived peak in $\delta^{18}O_{(diatom)}$ at 2.59 Ma. Sample resolution decreases after this interval, because of the difficulties in obtaining very clean samples,

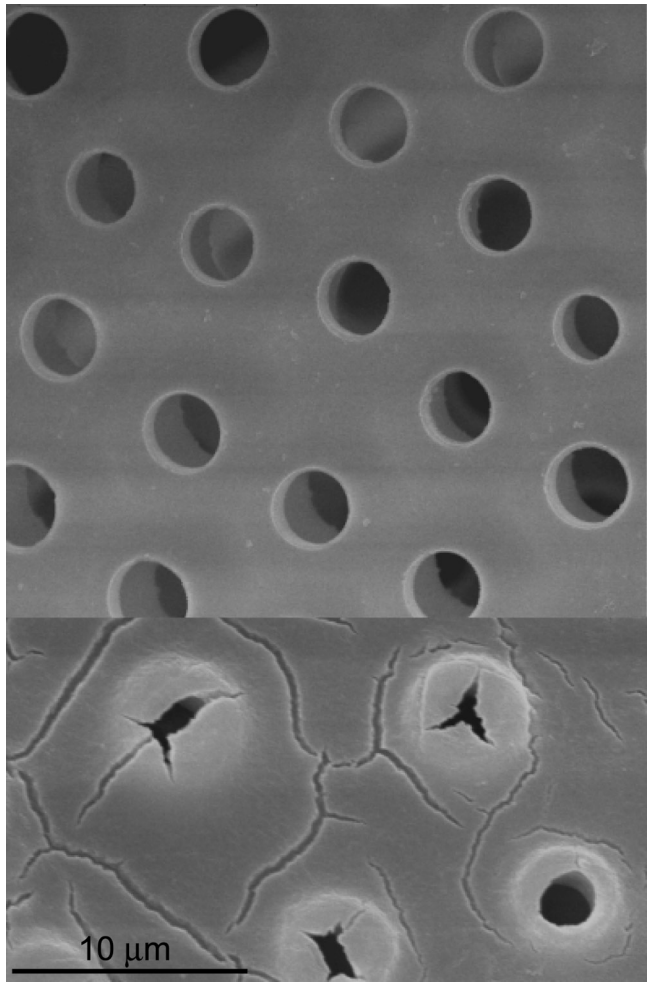


**Figure 5.** Typical, clean, scanning electron microscope (SEM) images of diatom material analyzed for oxygen isotopes at ODP site 882 showing the complete removal of adhering clays and other forms of contamination.

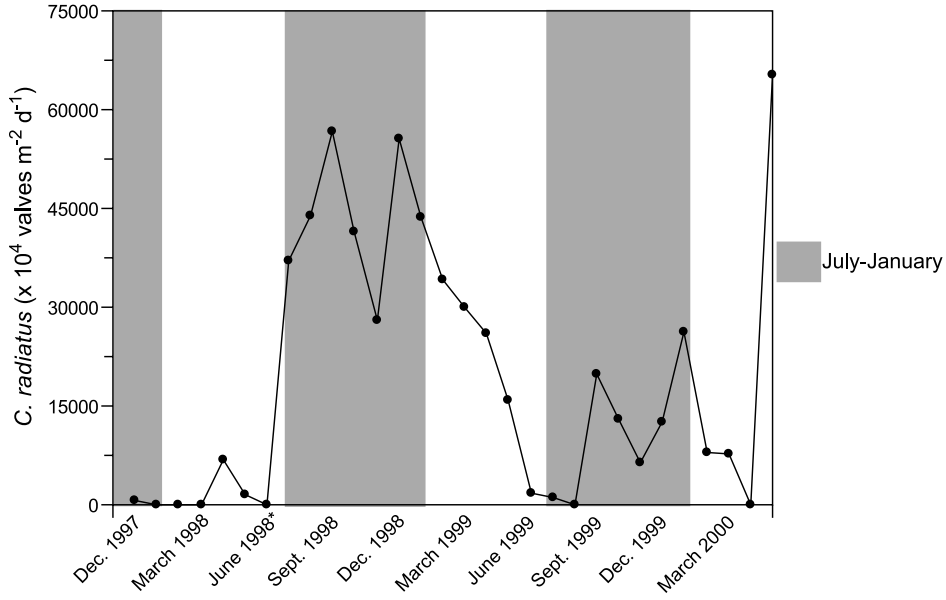


**Figure 6.** Mean monthly *C. radiatus* flux levels at station 50N (50°N, 165°E) in the northwest Subarctic Pacific from December 1997 to May 2000 (data adapted from *Onodera et al.* [2005]). Fluxes are dominated by significantly higher blooms in the late summer to early winter periods which, combined with additional data showing *C. marginatus* to bloom in the autumn/early winter period [*Takahashi*, 1986; *Takahashi et al.*, 1996; *Onodera et al.*, 2005; K. Takahashi and J. Onodera, personal communication, 2005], indicates the $\delta^{18}O_{(diatom)}$ signal extracted in this study to be representative of autumn/early winter oceanic conditions.

with an overall $\delta^{18}O_{(diatom)}$ decrease of 7.7‰ to 34.9‰ observed by 2.4 Ma.

## 4. Discussion

### 4.1. Extraction of Low Species Diversity, Pure Diatom Material in Marine Samples

[13] Obtaining pure diatom material for isotope analysis is challenging when diatoms are intermixed with similar sized clay and silt grains. Consequently, $\delta^{18}O_{(diatom)}$ is highly sensitive to the degree of sample contamination, particularly when sample purify falls below 90% [*Morley et al.*, 2004]. Several techniques have been suggested in the past [e.g., *Shemesh et al.*, 1995; *Morley et al.*, 2004; *Rings et al.*, 2004; *Lamb et al.*, 2005] but success with one particular diatom extraction technique is no guide to success with material from another site. Here we suggest a three-stage methodology for the purification of marine diatom samples for isotope analysis similar to that proposed for lacustrine samples by *Morley et al.* [2004] (Figure 3). We suggest that this technique is ideal for sites possessing large marine diatoms and has significant potential in extracting clean samples which contain low diatom species diversity and species that bloom over a single season. This is crucial if we are to improve the errors associated with diatom isotope studies which are almost an order of magnitude higher at present than those from isotope analyses of authigenic and carbonate fossils. Consequently, we emphasize the importance of visual analysis of the sediment prior to the first sieving stage as a precursor to selecting sieve fraction sizes in order to ensure low sample species diversity. A balance is needed though between reducing the number of species and ensuring sufficient material is extracted for isotope analysis.

### 4.2. Reliability of the $\delta^{18}O_{(diatom)}$ Record at ODP Site 882

[14] Analysis of $\delta^{18}O_{(diatom)}$ for paleoclimatic and paleoenvironmental purposes is a comparatively recent development. As such, consideration is required of issues which may complicate or affect the reliability of the $\delta^{18}O_{(diatom)}$ signal including: clay/silt contamination, seasonal dilution of $\delta^{18}O_{(diatom)}$, interspecies fractionation effects and secondary isotope exchange. As highlighted in section 3 and Figure 5, visual analysis of all samples indicates minimal/no contamination of samples with nondiatom material. The presence of high $\delta^{18}O_{(diatom)}$ values in all samples further demonstrates this since the $\delta^{18}O$ of clays and silts are usually significantly lower than the $\delta^{18}O_{(diatom)}$ values obtained here (common values are approximately 10–12‰). Previous diatom isotope studies have also been hampered by the $\delta^{18}O_{(diatom)}$ signal being diluted by the mixing of spring and autumnal blooming diatoms [e.g., *Raubitschek et al.*, 1999; *Leng et al.*, 2001]. Here this issue is resolved by the extraction of *C. marginatus* and *C. radiatus* which both predominantly bloom in the autumn/early winter period [*Takahashi*, 1986; *Takahashi et al.*, 1996; *Onodera et al.*, 2005; K. Takahashi and J. Onodera, personal communication, 2005] (Figure 6). Consequently, we can be confident that our $\delta^{18}O_{(diatom)}$ signal is independent of spring surface water conditions.

[15] A significant uncertainty for $\delta^{18}O_{(diatom)}$-based studies resolves over the potential for diatom interspecies

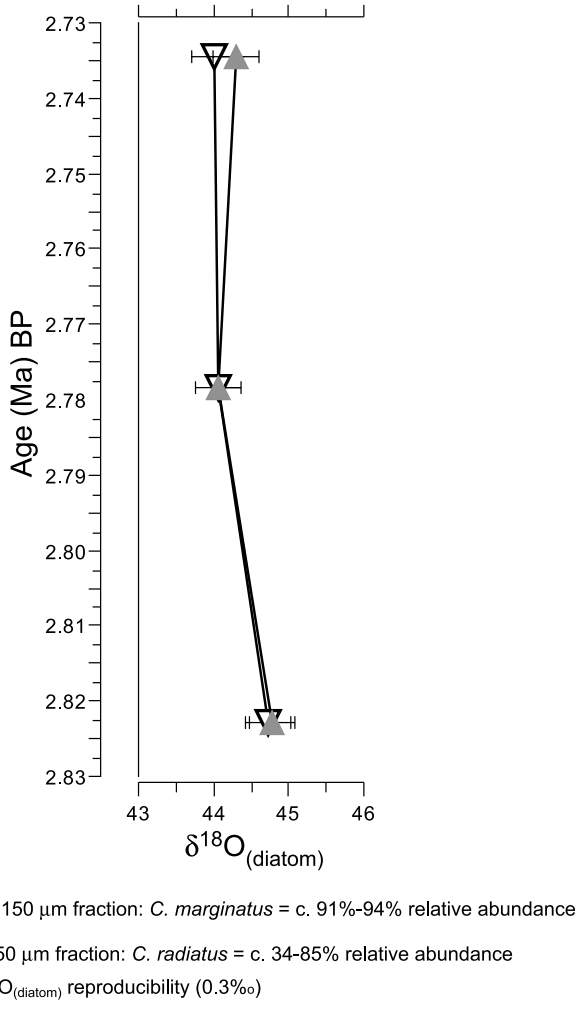


**Figure 7.** The $\delta^{18}O_{(diatom)}$ measurements with mean reproducibility of 0.3‰ for three pairs of same depth samples from the 75–150 μm and >150 μm size fractions that contain different relative proportions of *C. marginatus* and *C. radiatus*. Whereas the 75–150 μm fraction is dominated by *C. marginatus*, the >150 μm fraction is predominantly made up of *C. radiatus*. Similar results between size fractions at all levels, within the limits of reproducibility, indicate no vital effects between the two species.

fractionation effects. To date, no published evidence exists to indicate the presence of such effects in diatoms but caution is required given the current limited number of published data sets [*Shemesh et al.*, 1995; *Rosqvist et al.*, 1999]. Several lines of evidence suggest that changes in the relative abundance of the two diatom species are not responsible for variations in $\delta^{18}O$. Analysis of different size fractions, which contain different relative proportion of *C. marginatus* and *C. radiatus* reveal results within the mean 0.3‰ analytical error for $\delta^{18}O_{(diatom)}$ (Figures 4 and 7). Furthermore, species shifts and isotope shifts are not coeval. While the large decrease in $\delta^{18}O_{(diatom)}$ begins at 2.73 Ma (102.99 (meters below seafloor) mbsf), the major change in the relative proportion of silica biovolume contributed by *C. marginatus* and *C. radiatus* occurs much later at 2.71 Ma (102.66 mbsf). The approximately 5–10‰ shifts in $\delta^{18}O_{(diatom)}$ throughout the analyzed section are also sufficiently large to blur any potential noise from interspecies vital effects, since these are approximately 2–3‰ in foraminifera, while correlation of individual species biovolume with $\delta^{18}O_{(diatom)}$ from circa 2.73 Ma produces a correlation coefficient of 0.16, suggesting no relationship.

[16] A final as yet unresolved issue stems from the culture experiments of *Brandriss et al.* [1998] and *Schmidt et al.* [1997, 2001] who demonstrate $\delta^{18}O_{(diatom)}$ values significantly below those modeled by the fossil-derived silica-water fractionation curve of *Juilliet-Leclerc and Labeyrie* [1987]. This has led to suggestions of possible successive isotopic exchanges between diatom amorphous silica and seawater/pore water which would limited the applicability of $\delta^{18}O_{(diatom)}$ measurements for reconstructive purposes particularly if the diatoms are subject to any form of diagenesis [*Schmidt et al.*, 1997, 2001]. The exact operation and mechanism of these secondary isotope exchange processes remains, at present, uncertain but are related to silica maturation in the sediment during the early stages of diatom frustule diagenesis [see *Schmidt et al.*, 2001]. While secondary isotope exchange may theoretically occur in the water column during settling [*Brandriss et al.*, 1998], recent experiments have found a lack of evidence to support this [*Schmidt et al.*, 2001]. If secondary isotope exchange, however, only affects the outer hydrous Si-OH layer of the diatom frustule, measurements of $\delta^{18}O_{(diatom)}$ can still be reliably used for paleoceanographic purposes [*Brandriss et al.*, 1998]. This is particularly true for measurements of $\delta^{18}O_{(diatom)}$ analyzed through stepwise fluorination, as performed here, in which the Si-OH layer is removed and only the inner, denser, Si-O-Si layer is used to extract $\delta^{18}O$. Recently, however, secondary isotope exchange has been suggested to be linked to the condensation of Si-OH groups within the frustule and the formation of Si-O-Si linkages, casting doubt over the reliability of $\delta^{18}O_{(diatom)}$ measurements [see *Schmidt et al.*, 2001]. As such, the existence of secondary isotope exchange would lead to the $\delta^{18}O_{(diatom)}$ signal being a combined signal reflective of both surface water and sediment pore water $\delta^{18}O$. We are confident here, however, that there is no or only very minimal secondary isotope exchange influence on the diatom frustules and that $\delta^{18}O_{(diatom)}$ can be reliably used to monitor surface water changes. First, the maximum deep water $\delta^{18}O$ shift as record by benthic foraminifera, and hence change in sediment pore water, across the development of NHG is on the order of approximately 0.4‰ [*Shackleton et al.*, 1995]. With frequent $\delta^{18}O_{(diatom)}$ fluctuations of approximately 5–10‰ throughout the analyzed period, the possibility and importance of changes in pore water $\delta^{18}O$ in controlling the large and major shift in $\delta^{18}O_{(diatom)}$ can be discounted. From this, we can also discount that variations in silica pore waters saturation through time control the diatom secondary isotope exchange, and hence the observed large shifts in $\delta^{18}O_{(diatom)}$, as large changes in $\delta^{18}O_{(diatom)}$ continue after 2.69 Ma when opal MAR are permanently low (Figure 8).

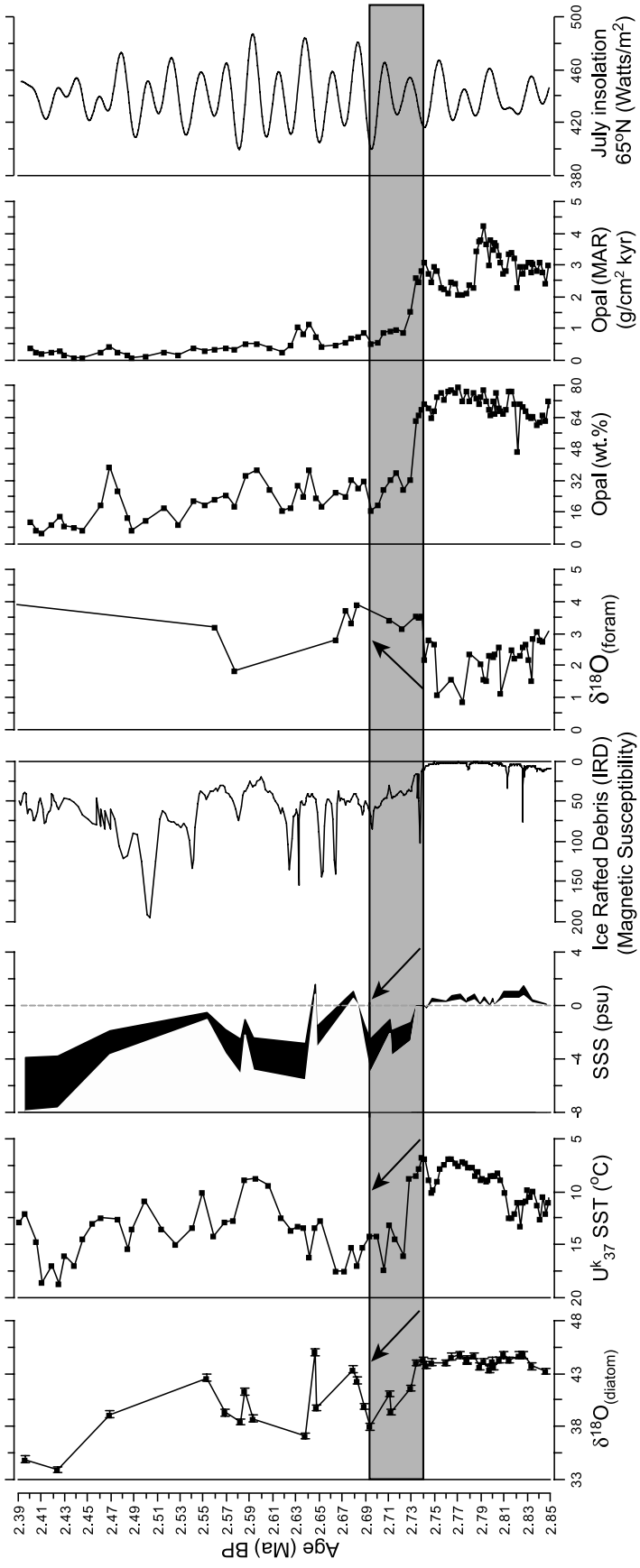


**Figure 8.** The $\delta^{18}O_{(diatom)}$ between 2.85 Ma and 2.39 Ma with calculated sea surface salinity (SSS) (relative to a SSS of 0 at 2.73 Ma), $U^{k}_{37}$ reconstructed sea surface temperature (SST) [*Haug et al.*, 2005], $\delta^{18}O_{(foram)}$ [*Maslin et al.*, 1995, 1996], ice-rafted debris (IRD) (magnetic susceptibility) [*Haug*, 1995], opal concentrations and opal mass accumulation rates (MAR) [*Haug*, 1995; *Haug et al.*, 1999], and July summer isolation at 65°N [*Berger and Loutre*, 1991]. Warming and freshening of surface waters at ODP site 882 from 2.73 Ma is indicated by decreases in $\delta^{18}O_{(diatom)}$, SSS, and opal MAR and increases in SST and IRD. Error bars on $\delta^{18}O_{(diatom)}$ measurements represent mean reproducibility of 0.3‰. Calculated SSS assumes a $\delta^{18}O_{(diatom)}$-temperature coefficient of −0.2‰/°C [*Brandriss et al.*, 1998; *Moschen et al.*, 2005]. The range of SSS values (shaded) reflects the uncertainty over the exact SSS:$\delta^{18}O$ relationship, which can vary between 1 and 2 depending on the oxygen isotope composition of the ocean and freshwater end-members.

What we cannot completely rule out is that minor shifts in $\delta^{18}O_{(diatom)}$ prior to 2.73 Ma may be potentially attributable to secondary isotope exchanges. However, given the extremely well preserved state of the diatom frustules analyzed here and the lack of any visible signs of diagenesis (see Figure 5), we assume that the role of secondary isotope exchange is limited throughout the analyzed interval. Results here therefore provide the first example of marine sediment samples analyzed for $\delta^{18}O_{(diatom)}$ which contain only two diatom species. Given our discussion above, we suggest that as changes in contamination, vital affects and secondary process have limited impact on the data presented here, we can interpret variations in $\delta^{18}O_{(diatom)}$ as changes in the surface waters. As such, $\delta^{18}O_{(diatom)}$ can be employed to reconstruct environmental changes in the northwest subarctic Pacific at the onset of major NHG in conjunction with the other existing proxy records for this site.

### 4.3. Onset of Major NHG at ODP Site 882

[17] Recently published coccolith $U^k_{37}$ measurements provide autumnal SST reconstructions for ODP site 882 between 2.85 and 2.39 Ma [*Haug et al.*, 2005]. Since $\delta^{18}O_{(diatom)}$ also indicates autumnal/early winter conditions in the photic zone, the two records can be combined to estimates changes in SSS (Figure 8). The benthic foraminifera isotope record at ODP site 846 [*Shackleton et al.*, 1995] is utilized to remove the Global Ice Volume component from $\delta^{18}O_{(diatom)}$ with changes in autumnal SST resolved using the $U^k_{37}$ record at ODP site 882 [*Haug et al.*, 2005]. The precise $\delta^{18}O_{(diatom)}$-temperature coefficient, however, remains uncertain with estimate ranging from $-0.2‰/°C$ to $-0.5‰/°C$ [*Juillet-Leclerc and Labeyrie*, 1987; *Shemesh et al.*, 1992; *Brandriss et al.*, 1998; *Moschen et al.*, 2005]. The most recent studies provide compelling evidence that the true coefficient is closer to $-0.2‰/°C$ [*Brandriss et al.*, 1998; *Moschen et al.*, 2005] which we use here. Further assumptions are also required as the relationship between SSS and oxygen isotopes can vary between 1:1 and 1:2 depending on the oxygen isotope composition of the oceanic and freshwater end-members [*Rohling*, 2000]. Defining the exact relationship is complicated by the large range of estimates for the $\delta^{18}O$ value of individual ice sheets [*Duplessy et al.*, 2002]. For the Eurasia and North American ice sheets estimated values for $\delta^{18}O$ at the Last Glacial Maximum varied from $-16‰$ to $-40‰$ and $-28‰$ and $-34‰$, respectively [*Duplessy et al.*, 2002]. To avoid making incorrect assumptions regarding the true relationship of SSS:$\delta^{18}O$, a range of SSS values are calculated here assuming SSS:$\delta^{18}O$ may have varied from 1 and 2. Changes in SSS relative to conditions at circa 2.73 Ma at the onset of major NHG using a $\delta^{18}O_{(diatom)}$-temperature coefficient of $-0.2‰/°C$ are displayed in Figure 8 and are used throughout the remainder of the discussion. For clarity, since we cannot fully discount a $\delta^{18}O_{(diatom)}$-temperature coefficient of $-0.5‰/°C$, alternative SSS calculations are displayed in Figure 9.

[18] The $\delta^{18}O_{(diatom)}$ variations of less than 1.4‰ prior to circa 2.73 Ma suggest the presence of comparatively uniform autumn/winter condition in the subarctic northwest Pacific prior to the onset of major NHG at 2.73 Ma Autumnal $U^k_{37}$ SST reconstructions of below 10°C verify this except from 2.83 Ma to 2.81 Ma when $U^k_{37}$ SST reconstructions indicate a 2°C increase to 13°C [*Haug et al.*, 2005] while no corresponding shift occurs in $\delta^{18}O_{(diatom)}$ (Figure 8). During this interval, SSS therefore appears to have increased by approximately 0.5–1 psu. However, the lack of any change in $\delta^{18}O_{(diatom)}$ during this period may also reflect an insensitivity of $\delta^{18}O_{(diatom)}$ to record small changes in SST. This would be related to the high $\delta^{18}O_{(diatom)}$ reproducibility in this study (up to 0.4‰ in some samples), combined with the possibility for diatom temperature fractionation coefficients to be as low as $-0.2‰/°C$ [*Brandriss et al.*, 1998; *Moschen et al.*, 2005]. Consequently, minor shifts in SST recorded in $\delta^{18}O_{(diatom)}$ would be inseparable from the analytical error. As highlighted above, the exact $\delta^{18}O_{(diatom)}$-temperature coefficient is at present uncertain though a value of $-0.2‰/°C$ appears to be close to the true value [*Moschen et al.*, 2005]. Using this, the 2°C disparity between $\delta^{18}O_{(diatom)}$ and $U^k_{37}$ SST is within our 0.4‰ $\delta^{18}O_{(diatom)}$ reproducibility. We cannot be certain therefore whether $\delta^{18}O_{(diatom)}$ over this interval is indicating a real increase in SSS or whether $\delta^{18}O_{(diatom)}$ is unsuitable for detecting low-magnitude variations in SST expect in instances where the reproducibility of isotope measurements is particularly good.

[19] At the onset of major NHG, circa 2.73 Ma, $\delta^{18}O_{(diatom)}$ decreases by 4.6‰ while $U^k_{37}$ reconstructed autumnal SST simultaneously increases by 7°C [*Haug et al.*, 2005], equating to an abrupt SSS freshening of 1.9 psu. (Figure 8). By 2.70 Ma, SSS had decreased by 2.5–5.1 psu relative to conditions at 2.73 Ma, equivalent to the modern day SSS difference between the northwest subarctic Pacific and the North Pacific/Tropical Pacific ocean [*Boyer et al.*, 2002]. With the autumnal blooming of *C. marginatus*, *C. radiatus* and coccoliths in the surface waters the changes observed here, indicating the development of a warm low-salinity pool of surface water, are entirely consistent with suggestions that the modern halocline in the subarctic Pacific developed at the beginning of major NHG [*Haug et al.*, 1999; *Sigman et al.*, 2004; *Haug et al.*, 2005]. In contrast, a no-halocline system would have been expected to initiate a cooling trend in $\delta^{18}O_{(diatom)}$ and $U^k_{37}$ with little or no change in SSS because of the unimpeded upwelling of NPDW. Evidence here therefore indicates increased seasonality at circa 2.73 Ma, together with reduced time lags between the atmosphere and oceanic temperature in the stratified surface waters, permitted the build up and maintenance of a pool of warm SST into the autumn/winter months [*Haug et al.*, 2005].

[20] Mechanisms for the initiation and development of the halocline in the region have previously been investigated by *Sigman et al.* [2004]. Increases in freshwater input alone are unlikely therefore to be the direct instigator in the development of the stratified system and the major reorganization of the water column which occurred at circa 2.73 Ma. However, as reiterated here by the reconstruction of a significant SSS decrease after 2.73 Ma and concordant increase in IRD (Figure 8), once established the stratified water column in the northwest Pacific would have become self-sustaining through further influxes of

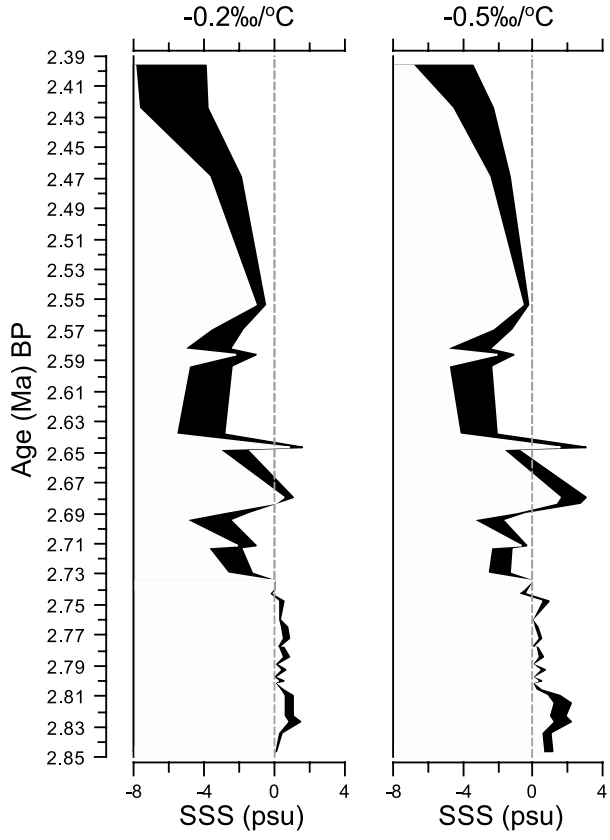


**Figure 9.** Calculated SSS in the northwest subarctic Pacific from 2.85 Ma to 2.39 Ma relative to a SSS of 0 psu at 2.73 Ma assuming different SSS:$\delta^{18}O$ values and $\delta^{18}O_{(diatom)}$-temperature coefficients. While the most likely scenario is for a $\delta^{18}O_{(diatom)}$ coefficient of $-0.2$‰/°C, a value of $-0.5$‰/°C cannot be ruled out. Furthermore, the value of SSS:$\delta^{18}O$ can potentially vary between 1 and 2 following changes in the oxygen isotope composition of the ocean and freshwater end-members, indicated by the range of SSS values (shaded). Regardless of the values used, SSS decreases in the region from 2.73 Ma by 1.18–3.75 psu indicating a significant reorganization in the water column at the onset of major Northern Hemisphere glaciation.

meltwater enhancing and reinforcing the existing salinity gradient between the surface and subsurface waters [*Sigman et al.*, 2004].

[21] Although the 2.6‰ increase in $\delta^{18}O_{(foram)}$ over the same interval [*Maslin et al.*, 1995, 1996] appears to conflict with the evidence provided by $\delta^{18}O_{(diatom)}$, $U^{k}_{37}$, opal MAR and $\delta^{15}N_{(bulk\ sediment)}$ (Figure 8), the two foraminifera species analyzed, *Globigerina bulloides* and *Neogloboquadrina pachyderma*, are unlikely to be reflective of autumnal/early winter sea surface conditions. Both species are primarily indicative of spring condition [*Kohfeld et al.*, 1996; *Ganssen and Kroon*, 2000; *Kuroyanagi et al.*, 2002; *Mohiuddin et al.*, 2002]. In particular, nearby sediment traps (50°01′N, 165°02′E) show these species to be most prevalent during spring although moderate fluxes do occur during the early winter months [*Kuroyanagi et al.*, 2002]. The $\delta^{18}O_{(foram)}$ increase would therefore be entirely consistent with expected spring condition in the region at the onset of NHG following halocline stratification given the globally cooler conditions and the lack of a thermocline and associated warm SST in the region during spring, which today results in SST of 2°–4°C (Figure 2). This would be enforced by the reduced phase lag that would exist between the ocean and the cooler air temperatures in the late winter/early spring months following stratification and by the input of cold freshwater from melting icebergs (Figure 8).

[22] More important and pertinent to our discussion is that $\delta^{18}O_{(foram)}$ is also highly susceptible to a species vertical migration and seasonal position in the water column [*Hemleben et al.*, 1989; *Kohfeld et al.*, 1996; *Kuroyanagi and Kawahata*, 2004]. Studies in the North Pacific indicate that *G. bulloides* and *N. pachyderma* live between 0 m and 300 m with a strong peak between 80 m and 200 m for *N. pachyderma* [*Kohfeld et al.*, 1996; *Kuroyanagi and Kawahata*, 2004]. *N. pachyderma* has also been found in the North Pacific to occur entirely below the pycnocline [*Kuroyanagi and Kawahata*, 2004]. Consequently, $\delta^{18}O_{(foram)}$ does not have the potential to reflect past SST within the autumnal/early winter thermocline, which lies today at approximately 50 m, even if the foraminifera's dominant growth season had switched from spring to autumn in the past (Figure 2). Instead, any autumn $\delta^{18}O_{(foram)}$ signal would be reflective of conditions beneath the stratification boundary which would again be expected to cool over this interval, in line with the observed increase in $\delta^{18}O_{(foram)}$, given the presence of globally colder conditions.

[23] The growth and establishment of the modern halocline system in the subarctic Pacific has significant consequences for our understanding of events at the beginning of NHG. Once established the stratification would restrict the nutrient rich bottom water from upwelling to the surface preventing the ventilation of carbon sequestered within the deep ocean to the atmosphere. Net release of carbon to the atmosphere is implied at the site prior to 2.73 Ma and the onset of NHG when low $\delta^{15}N_{(bulk\ sediment)}$ values reflect incomplete phytoplankton nutrient utilization [*Haug et al.*, 1999]. In contrast, after circa 2.73 Ma values of $\delta^{15}N_{(bulk\ sediment)}$ indicate a shift to higher nutrient utilization [*Haug et al.*, 1999]. Hence the region likely contributed toward driving cooler conditions across the globe, further permitting the growth of glaciers across the Northern Hemisphere and reinforcing stratification in the subarctic Pacific. Evidence here and by *Haug et al.* [2005] of a warm, approximately 17°–18°C, pool of water throughout the subarctic North Pacific Ocean from the onset of NHG onward also suggests the region may have acted as a key moisture source to the North American ice sheets. Furthermore, measurements of $\delta^{18}O_{(diatom)}$ indicate that high SST conditions could have prevailed in the North Pacific into the early winter months. Consequentially, the delivery of large quantities of moisture to North America could have continued at the time most favorable to glacial advance and snow accumulation.

[24] Following the development of the halocline system, large fluctuations in $\delta^{18}O_{(diatom)}$ and SSS remain apparent in the sedimentary record, particularly from 2.70 Ma onward. Given the current low-resolution nature of the $\delta^{18}O_{(diatom)}$ record we are unwilling to make any paleoceanographic interpretations at this time despite such evidence indicating continuing major environmental changes in the ocean surface waters. While, for example, the $\delta^{18}O_{(diatom)}$ and SSS records indicate a reversal to prehalocline conditions at 2.65 Ma, the lack of concordant changes in $U^k_{37}$ and opal MAR fails to support any suggestion of a shift back to a nonstratified system. Future work at this site will improve the temporal resolution of $\delta^{18}O_{(diatom)}$ measurements after circa 2.67 Ma, allowing the stability and presence of the stratification in the subarctic region and the relationship between $\delta^{18}O_{(diatom)}$ and $U^k_{37}$ to be monitored across the early glacial-interglacial cycles that follow the onset of major NHG. This will be complemented by attempts to extract spring blooming diatoms to create a $\delta^{18}O_{(diatom)}$ record of spring water column conditions across this interval in the region. At present, generating sufficiently clean samples free of autumnal blooming diatoms is proving problematic.

## 5. Conclusion

[25] Results here provide the first $\delta^{18}O_{(diatom)}$ curve across the onset of major NHG. By analyzing season specific pure diatom samples for oxygen isotope ratios, we have found strong evidence to support and reinforce claims that the modern halocline system developed in the subarctic northwest Pacific from circa 2.73 Ma. Confirmed by recently published $U^k_{37}$ data that indicate a simultaneous 7°C increase in SST, a plausible mechanism now exists by which adequate supplies of moisture could have been delivered to the growing North American ice sheets [*Haug et al.*, 2005]. The onset of stratification further supports claims that the region may have made a significant contribution toward lowering atmospheric $CO_2$ concentrations by preventing deep water ventilation [*Haug et al.*, 1999]. In contrast to $\delta^{18}O_{(diatom)}$ and $U^k_{37}$, the increase in $\delta^{18}O_{(foram)}$ most likely indicates oceanographic changes either in spring and/or below the water column stratification in spring or autumn. The use of $\delta^{18}O_{(diatom)}$ alongside $\delta^{18}O_{(foram)}$ therefore highlights the considerable potential that both proxies contain, when utilized together, in aiding our understanding and interpretation of past climatic events. Consequently, $\delta^{18}O_{(diatom)}$ should not be considered solely as an alternative proxy in regions where foraminifera and other calcium carbonate fossil are not present in the sedimentary record.

[26] **Acknowledgments.** The authors would like to thank John Barron and Cathy Stickley for advice on taxonomic identification in addition to Jonaotaro Onodera and Kozo Takahashi for the discussion on *C. radiatus* and *C. marginatus* seasonal fluxes while also providing and giving permission to present the *C. radiatus* diatom flux data from station 50°N in Figure 6. We also acknowledge and thank Gavin Simpson (ECRC) for providing much of the R script used to create the SST and SSS plots in Figure 2. Additional thanks are given to the two anonymous reviewers for their constructive comments and to the Ocean Drilling Program (ODP) for making available the sample material. This study was carried out during a NERC Ph.D. studentship award to G.E.A.S. (NER/S/A/2004/12193).

## References

Berger, A., and M. F. Loutre (1991), Insolation values for the climate of the last 10 million years, *Quat. Sci. Rev.*, *10*, 297–317.

Bosilovich, M. G. (2002), On the vertical distribution of local and remote sources of water for precipitation, *Meteorol. Atmos. Phys.*, *80*, 31–41.

Boyer, T. P., C. Stephens, J. I. Antonov, M. E. Conkright, R. A. Locarnini, T. D. O'Brien, and H. E. Garcia (2002), *World Ocean Atlas 2001*, vol. 2, *Salinity*, *NOAA Atlas NESDIS 50* [CD-ROM], edited by S. Levitus, 165 pp., NOAA, Silver Spring, Md.

Brandriss, M. E., J. R. O'Neil, M. B. Edlund, and E. F. Stoermer (1998), Oxygen isotope fractionation between diatomaceous silica and water, *Geochim. Cosmochim. Acta*, *62*, 1119–1125.

Clayton, R. N., and T. K. Mayeda (1963), The use of bromine pentafluoride in the extraction of oxygen from oxide and silicates for isotope analysis, *Geochim. Cosmochim. Acta*, *27*, 43–52.

Duplessy, J.-C., L. Labeyrie, and C. Waelbroeck (2002), Constraints on the oxygen isotopic enrichment between the Last Glacial Maximum and the Holocene: Paleoceanographic implications, *Quat. Sci. Rev.*, *21*, 315–330.

Ganssen, G. M., and D. Kroon (2000), The isotopic signature of planktonic foraminifera from NE Atlantic surface sediments: Implications for the reconstruction of past oceanic conditions, *J. Geol. Soc. London*, *157*, 693–699.

Gargett, A. E. (1991), Physical processes and the maintenance of nutrient-rich euphotic zones, *Limnol. Oceanogr.*, *36*, 1527–1545.

Haug, G. H. (1995), The evolution of northwest Pacific Ocean over the last 6 Ma: ODP LEG 145, Ph.D. thesis, 200 pp., Univ. of Kiel, Kiel, Germany.

Haug, G. H., and R. Tiedemann (1998), Effect of the formation of the Isthmus of Panama on Atlantic Ocean thermohaline circulation, *Nature*, *393*, 673–676.

Haug, G. H., D. M. Sigman, R. Tiedemann, T. F. Pedersen, and M. Sarnthein (1999), Onset of permanent stratification in the subarctic Pacific Ocean, *Nature*, *401*, 779–782.

Haug, G. H., R. Tiedemann, R. Zahn, and A. Christina Ravelo (2001), Role of Panama uplift on oceanic freshwater balance, *Geology*, *29*, 207–210.

Haug, G. H., et al. (2005), North Pacific seasonality and the glaciation of North America 2.7 million years ago, *Nature*, *433*, 821–825.

Hemleben, C., M. Spindler, and O. R. Anderson (1989), *Modern Planktonic Foraminifera*, 363 pp., Springer, New York.

Hillebrand, H., C.-D. Dürselen, D. Kirschtel, U. Pollingher, and T. Zohary (1999), Biovolume calculation for pelagic and benthic microalgae, *J. Phycol.*, *35*, 403–424.

Juillet-Leclerc, A. (1986), Cleaning process for diatomaceous samples, in *Proceedings of the 8th Diatom Symposium*, edited by M. Ricard, pp. 733–736, Koeltz Sci., Koenigstein, Germany.

Juillet-Leclerc, A., and L. Labeyrie (1987), Temperature dependence of the oxygen isotopic fractionation between diatom silica and water, *Earth Planet. Sci. Lett.*, *84*, 69–74.

Kleiven, H. F., E. Jansen, T. Fronval, and T. M. Smith (2002), Intensification of Northern Hemisphere glaciations in the circum Atlantic region (3.5–2.4 Ma)-Ice-rafted detritus evidence, *Palaeogeogr. Palaeoclimatol. Palaeoecol.*, *184*, 213–223.

Kohfeld, K. E., R. G. Fairbanks, S. L. Smith, and I. D. Walsh (1996), *Neogloboquadrina pachyderma* (sinistral coiling) as paleoceanographic tracers in polar oceans: Evidence from Northeast Water Polynya plankton tows, sediment traps, and surface sediments, *Paleoceanography*, *11*, 679–699.

Koster, R., J. Jouzel, R. Suozzo, G. Russell, W. Broecker, D. Rind, and P. Eagleson (1986), Global sources of local precipitation as determined by the NASA/GISS GCM, *Geophys. Res. Lett.*, *13*, 121–124.

Kuroyanagi, A., and H. Kawahata (2004), Vertical distribution of living planktonic foraminifera in the seas around Japan, *Marine Micropaleontol.*, *53*, 173–196.

Kuroyanagi, A., H. Kawahata, H. Nishi, and M. C. Honda (2002), Seasonal changes in planktonic foraminifera in the northwestern North Pacific Ocean: Sediment trap experiments from subarctic and subtropical gyres, *Deep Sea Res., Part II*, *49*, 5627–5645.

Lamb, A. L., M. J. Leng, H. J. Sloane, and R. J. Telford (2005), A comparison of the palaeoclimatic signals from diatom oxygen isotope ratios and carbonate oxygen isotope ratios from a low latitude crater lake, *Palaeogeogr. Palaeoclimatol. Palaeoecol.*, *223*, 290–302.

Lear, C. H., Y. Rosenthal, and J. D. Wright (2003), The closing of a seaway: Ocean water masses and global climate change, *Earth Planet. Sci. Lett.*, *210*, 425–436.

Leng, M. J., and P. A. Barker (2006), A review of the oxygen isotope composition of lacustrine diatom silica for paleoclimate reconstruction, *Earth Sci. Rev.*, in press.

Leng, M. J., P. Barker, P. A. Greenwood, N. Roberts, and J. Reed (2001), Oxygen isotope analysis of diatom silica and authigenic calcite from Lake Pinarbasi, Turkey, *J. Paleolimnol.*, *25*, 343–349.

Li, X., S. A. Berger, M. F. Loutre, M. A. Maslin, G. H. Haug, and R. Tiedemann (1998), Simulating late Pliocene Northern Hemisphere climate with the LLN 2-D model, *Geophys. Res. Lett.*, *25*, 915–918.

Maslin, M. A., G. H. Haug, M. Sarnthein, R. Tiedemann, H. Erlenkeuser, and R. Stax (1995), Northwest Pacific site 882: The initiation of major Northern Hemisphere glaciation, *Proc. Ocean Drill. Program Sci. Results*, *145*, 315–329.

Maslin, M. A., G. H. Haug, M. Sarnthein, and R. Tiedemann (1996), The progressive intensification of Northern Hemisphere glaciation as seen from the North Pacific, *Geol. Rundsch.*, *85*, 452–465.

Maslin, M. A., X-S. Li, M.-F. Loutre, and A. Berger (1998), The contribution of orbital forcing to the progressive intensification of Northern Hemisphere glaciation, *Quat. Sci. Rev.*, *17*, 411–426.

Mikkelsen, N., L. Labeyrie, and W. H. Berger (1978), Silica oxygen isotopes in diatoms: A 20000 yr record in deep-sea sediments, *Nature*, *271*, 536–538.

Mochizuki, M., N. Shiga, M. Saito, K. Imai, and Y. Nojiri (2002), Seasonal changes in nutrients, chlorophyll a and the phytoplankton assemblages of the western subarctic gyre in the Pacific Ocean, *Deep Sea Res., Part II*, *49*, 5421–5439.

Mohiuddin, M. M., A. Nishimura, Y. Tanaka, and A. Shimamoto (2002), Regional and interannual productivity of biogenic components and planktonic foraminiferal fluxes in the northwestern Pacific Basin, *Mar. Micropaleontol.*, *45*, 57–82.

Mohiuddin, M. M., A. Nishimura, and Y. Tanaka (2005), Seasonal succession, vertical distribution, and the dissolution of planktonic foraminifera along the Subarctic Front: Implications for paleoceanographic reconstruction in the northwestern Pacific, *Mar. Micropaleontol.*, *55*, 129–156.

Morley, D. W., M. J. Leng, A. W. Mackay, H. J. Sloane, P. Rioual, and R. W. Battarbee (2004), Cleaning of lake sediment samples for diatom oxygen isotope analysis, *J. Paleolimnol.*, *31*, 391–401.

Morley, D. W., M. J. Leng, A. W. Mackay, and H. J. Sloane (2005), Late Glacial and Holocene environmental change in the Lake Baikal region documented by oxygen isotopes from diatom silica, *Global Planet. Change*, *46*, 221–233.

Moschen, R., A. Lücke, and G. Schleser (2005), Sensitivity of biogenic silica oxygen isotopes to changes in surface water temperature and palaeoclimatology, *Geophys. Res. Lett.*, *32*, L07708, doi:10.1029/2004GL022167.

Ohkouchi, N., K. Kawamura, H. Kawahata, and H. Okada (1999), Depth ranges of alkenone production in the central Pacific Ocean, *Global Biogeochem. Cycles*, *13*, 695–705.

Onodera, J., and K. Takahashi (2005), Silicoflagellate fluxes and environmental variations in the northwestern North Pacific during December 1997–May 2000, *Deep Sea Res., Part I*, *52*, 371–388.

Onodera, J., K. Takahashi, and M. C. Honda (2005), Pelagic and coastal diatom fluxes and the environmental changes in the northwestern North Pacific during 1997–2000, *Deep Sea Res., Part II*, *52*, 2218–2239.

Pagani, M., K. H. Freeman, N. Ohkouchi, and K. Caldeira (2002), Comparison of water column [$CO_{2aq}$] with sedimentary alkenone-based estimates: A test of the alkenone-$CO_2$ proxy, *Paleoceanography*, *17*(4), 1069, doi:10.1029/2002PA000756.

Prueher, L. M., and D. K. Rea (2001), Volcanic triggering of late Pliocene glaciation: Evidence from the flux of volcanic glass and ice-rafted debris to the North Pacific Ocean, *Palaeogeogr. Palaeoclimatol. Palaeoecol.*, *173*, 215–230.

Raubitschek, S., A. Lücke, and G. H. Schleser (1999), Sedimentation patterns of diatoms in Lake Holzmaar, Germany - (on the transfer of climate signals to biogenic silica oxygen isotope proxies), *J. Paleolimnol.*, *21*, 437–448.

Ravelo, A. C., D. H. Andreasen, M. Lyle, A. O. Lyle, and M. W. Wara (2004), Regional climate shifts caused by gradual cooling in the Pliocene epoch, *Nature*, *429*, 263–267.

Raymo, M. E. (1994), The Himalayas, organic-carbon burial, and climate in the Miocene, *Paleoceanography*, *9*, 399–404.

Rea, D. K., I. A. Basov, D. W. Scholl, and J. F. Allan (Eds.) (1995), *Proceedings of the Ocean Drilling Program*, *Scientific Results*, vol. 145, Ocean Drill. Program, College Station, Tex.

Rings, A., A. Lücke, and G. H. Schleser (2004), A new method for the quantitative separation of diatom frustules from lake sediments, *Limnol. Oceanogr. Methods*, *2*, 25–34.

Rohling, E. J. (2000), Paleosalinity: Confidence limits and future applications, *Mar. Geol.*, *163*, 1–11.

Rosqvist, G. C., M. Rietti-Shati, and A. Shemesh (1999), Late glacial to middle Holocene climate record of lacustrine biogenic silica oxygen isotopes from a Southern Ocean island, *Geology*, *27*, 967–970.

Ruddiman, W. F., and M. E. Raymo (1988), Northern Hemisphere climate regimes during the past 3 Ma: Possible tectonic connections, *Philos. Trans. R. Soc. London, Ser. B*, *318*, 411–430.

Schmidt, M., R. Botz, P. Stoffers, T. Anders, and G. Bohrmann (1997), Oxygen isotopes in marine diatoms: A comparative study of analytical techniques and new results on the isotopic composition of recent marine diatoms, *Geochim. Cosmochim. Acta*, *61*, 2275–2280.

Schmidt, M., R. Botz, D. Rickert, G. Bohrmann, S. R. Hall, and S. Mann (2001), Oxygen isotope of marine diatoms and relations to opal-A maturation, *Geochim. Cosmochim. Acta*, *65*, 201–211.

Shackleton, N. J., M. A. Hall, and D. Pate (1995), Pliocene stable isotope stratigraphy of site 846, *Proc. Ocean Drill. Program Sci. Results*, *138*, 337–357.

Shemesh, A., C. D. Charles, and R. G. Fairbanks (1992), Oxygen isotopes in biogenic silica: Global changes in ocean temperature and isotopic composition, *Science*, *256*, 1434–1436.

Shemesh, A., L. H. Burckle, and J. D. Hays (1995), Late Pleistocene oxygen isotope records of biogenic silica from the Atlantic sector of the Southern Ocean, *Paleoceanography*, *10*, 179–196.

Sigman, D. M., S. L. Jaccard, and G. H. Haug (2004), Polar ocean stratification in a cold climate, *Nature*, *428*, 59–63.

Stephens, C., J. I. Antonov, T. P. Boyer, M. E. Conkright, R. A. Locarnini, T. D. O'Brien, and H. E. Garcia (2002), *World Ocean Atlas 2001*, vol. 1, *Temperature* [CD-ROM], *NOAA Atlas NESDIS 49*, edited by S. Levitus, 165 pp., NOAA, Silver Spring, Md.

Tabata, S. (1975), The general circulation of the Pacific Ocean and a brief account of the oceanographic structure of the North Pacific Ocean. part I, Circulation and volume transports, *Atmosphere*, *13*, 134–168.

Takahashi, K. (1986), Seasonal fluxes of pelagic diatoms in the subarctic Pacific, 1982–1983, *Deep Sea Res., Part A*, *33*, 1225–1251.

Takahashi, K., K. Hisamichi, M. Yanada, and Y. Maita (1996), Seasonal changes of marine phytoplankton productivity: A sediment trap study (in Japanese), *Kaiyo Mon.*, *10*, 109–115.

Tiedemann, R., and G. H. Haug (1995), Astronomical calibration of cycle stratigraphy for site 882 in the northwest Pacific, *Proc. Ocean Drill. Program Sci. Results*, *145*, 283–292.

Ueno, H., and I. Yasuda (2000), Distribution and formation of the mesothermal structure (temperature inversion) in the North Pacific subarctic region, *J. Geophys. Res.*, *105*, 16885–16897.

Zachos, J., M. Pagani, L. Sloan, E. Thomas, and K. Billups (2001), Trends, rhythms and aberrations in global climate 65 Ma to present, *Science*, *292*, 686–693.

G. H. Haug, Geoforschungszentrum Potsdam, Telegrafenberg, 14473 Potsdam, Germany.

M. J. Leng and H. J. Sloane, NERC Isotope Geosciences Laboratory, British Geological Survey, Keyworth, NG12 5GG Nottingham, UK.

M. A. Maslin and G. E. A. Swann, Environmental Change Research Centre, Department of Geography, University College London, 26 Bedford Way, WC1H 0AP London, UK. (g.swann@ucl.ac.uk)